Monte Carlo investigations of hexadecane films on a metal substrate

Sundaram Balasubramanian, Michael L. Klein, and J. Ilja Siepmann

Citation: The Journal of Chemical Physics **103**, 3184 (1995); doi: 10.1063/1.470251
View online: http://dx.doi.org/10.1063/1.470251
View Table of Contents: http://scitation.aip.org/content/aip/journal/jcp/103/8?ver=pdfcov
Published by the AIP Publishing

Monte Carlo investigations of hexadecane films on a metal substrate

Sundaram Balasubramanian and Michael L. Klein
Department of Chemistry, University of Pennsylvania, Philadelphia, Pennsylvania 19104-6323

J. Ilja Siepmann
Department of Chemistry, University of Minnesota, Minneapolis, Minnesota 55455-0431

(Received 14 April 1995; accepted 17 May 1995)

The structural properties of liquid *n*-hexadecane films, ranging in thickness from 1 to 4 nm and adsorbed on a flat metal (Au) surface, have been studied by the configurational-bias Monte Carlo method. Over the temperature range 350 K to 650 K, the substrate was found to induce a well-defined layering of the molecules for the portion of the film closest to the surface. Even at the highest temperature, this layering extends beyond a monolayer. In the surface layer, molecules are predominantly oriented with their long axes and their backbone zig–zag planes parallel to the substrate. Molecules close to the surface are also characterized by fewer *gauche* defects and are more densely packed than those present in the bulk region of the film. At a given temperature, the density and the characteristics of the molecules in the first adsorbed layer are substantially independent of the total thickness of the film. With increasing temperature, the layering diminishes and molecules in the first layer exhibit properties closer to those of the bulk liquid at a lower temperature. Comparisons are made with experiments and previous simulation studies on related systems. © *1995 American Institute of Physics.*

I. INTRODUCTION

The structure and dynamics of confined fluids have been subjects of intense experimental and theoretical study over the past decade.[1–15] Interest in these systems has been triggered by their wide range of technological applications, for example in lubrication and catalysis. Liquids under confinement exhibit properties different from those in the bulk.[1] Under strong adsorption, or at high pressure, molecules tend to approach close packing, leading to a higher-than-bulk-liquid density near the surface. Liquid molecules in the vicinity of the confining surfaces have been found to order as layers parallel to the surface.[3,9,10] At distances beyond the range of strong liquid–substrate interactions, properties corresponding to the bulk liquid are regained. A variety of liquid films composed of molecules ranging from spherical Lennard-Jones particles[6] to more complex long chain alkanes on metal[9–11] and graphite surfaces[16–18] have been studied using simulation methods. In particular, monolayers of long chain alkane molecules are observed to form lamellar phases on graphite[19–21] and are thus excellent candidates to study phase transitions in two dimensions. The significant differences in the static structure of these physisorbed liquid films manifests itself in their dynamics also. The films are found to support shear stress and the effective viscosity near the surface seems to be much higher than the bulk viscosity.[22,23] Conversely, they exhibit a yield point in the variation of shear stress with time which points to their solidlike nature.[5,12] Since the usual ''no-slip'' boundary conditions used in solving the Navier–Stokes equations may no longer be applied to these systems, Bocquet and Barrat[24] have proposed a boundary condition which allows for a velocity slip at the liquid–solid interface. Recent simulation studies[25] have identified a nonexponential relaxation of the time correlation functions for molecules close to the surface, typical of a ''glassy'' state. The study of such films is thus important in understanding the microscopic details of friction and 2D phase transitions.

A series of experiments performed by Israelachvili and co-workers to measure the surface forces of alkane films between mica surfaces have yielded oscillatory force profiles[3] as a function of surface separation. These force profiles indicated a layering of the molecules under confinement and it has been speculated that the alkane chains tend to lie with their long axes parallel to the surface.[3] This view has been supported by recent molecular dynamics simulations of octane films confined by the alkyl tails of a self assembled monolayer[14] and of a hexadecane film constrained between two flat metal surfaces.[10] Furthermore, simulations have detected similar layering for alkanes adsorbed on graphite.[16] Thus, the finding that chain molecules in liquid films form layers on the surface is now well established. However, additional systematic studies are justified to obtain a more detailed picture of the role of structure and conformation of molecules in these organic films. In this article, we investigate the influence of film thickness and temperature on the structural properties of linear long-chain alkane ($C_{16}H_{34}$) films adsorbed on a flat, metal surface. The long relaxation times exhibited by chains close to the surfaces[7,22] may lead to equilibration problems when conventional molecular dynamics simulation techniques are used. To circumvent this problem, we have used the configurational-bias Monte Carlo technique[26–28] which has been shown to be powerful for the study of long flexible molecules. Particular care has been taken to check that well-equilibrated films were obtained. The present investigation sets the stage for a systematic investigation of the effects of molecular architecture on film properties.

 0021-9606/95/103(8)/3184/12/$6.00

TABLE I. Details of the potential model used in this work. Parameters for unlike bead interactions were obtained by the following rule: $\epsilon_{ij}=(\epsilon_i\epsilon_j)^{1/2}$. The interaction potentials between alkane beads were cutoff at 13.8 Å as in the earlier work of ours (Ref. 31). No tail corrections were employed in view of the "open" nature of the system under investigation.

Interaction	Potential function	Parameters
Bond stretching (Ref. 59)	$U_{\text{stretch}}(r_{ij})=0.5k_r(r_{ij}-r_0)^2$	$k_r=452\,900$ K Å^{-2} $r_0=1.54$ Å
Bond bending (Ref. 60)	$U_{\text{bend}}(\theta_i)=0.5k_\theta(\theta_i-\theta_0)^2$	$k_\theta=62\,500$ K rad^{-2} $\theta_0=114°$
Torsional motion (Ref. 61)	$U_{\text{torsion}}(\phi_i)=a_1(1+\cos\phi_i)+$ $a_2(1-\cos(2\phi_i))+a_3(1+\cos(3\phi_i))$	$a_1=355.03$ K $a_2=-68.19$ K $a_3=791.32$ K
Non-bonded (Ref. 31)	$U_{\text{LJ}}(r_{ij})=4\epsilon[(\sigma_{ij}/r_{ij})^{12}-(\sigma_{ij}/r_{ij})^6]$	$\sigma_{CH_3}=\sigma_{CH_2}=3.93$ Å $\epsilon_{CH_3}=114.0$ K $\epsilon_{CH_2}=47.0$ K
Substrate (Ref. 34)	$U_{\text{subs}}(z)=A(z-z_0)^{-12}-C(z-z_0)^{-3}$	$A_{CH_3}=3.41\times10^7$ K Å^{12} $A_{CH_2}=2.80\times10^7$ K Å^{12} $C_{CH_3}=2.08\times10^4$ K Å^3 $C_{CH_2}=1.71\times10^4$ K Å^3 $z_0^{CH_3}=z_0^{CH_2}=0.86$ Å

II. MOLECULAR MODEL

The Monte Carlo (MC) method is particularly suited for the study of systems consisting of long, flexible chain molecules because, unlike the molecular dynamics (MD) method, it is not tied to the natural time evolution of the system which is likely to be retarded by slowest conformational changes. In the MC method, "smart" moves can be generated which sample the configurational space of the system in an efficient manner.[29] In the present problem, the recently developed configurational-bias Monte Carlo (CBMC) method[26–28] has been employed for this purpose. In the CBMC technique, large-scale conformational rearrangements of flexible molecules can occur in a single trial move. During a CBMC move, an entire chain molecule or part thereof is discarded and then regrown under the influence of its local environment. Thus, unfavorable conformations of the chain can be avoided. The bias introduced in the sampling is removed by properly adjusting the usual Metropolis acceptance criterion.[26] Over the last few years, the CBMC method has been successfully applied to a variety of molecular systems which are not readily amenable to conventional simulation techniques.[15,30,31]

The *n*-hexadecane molecules in the present study were considered to be fully flexible (i.e., bond stretching, angle bending, and dihedral motion were included) and to consist of united atoms of methyl and methylene groups which hereafter will be referred to as "beads." The potentials for the nonbonded interactions between the beads, and those governing the angle bending and torsional motion were the same as in the model which we recently derived from calculations of the vapor–liquid phase diagrams of normal alkanes.[31,32] This model has been supplemented by a harmonic bond vibration term which allows us to perform both MD and MC simulations using the identical description of the molecules.[33] The details of our potential model are given in Table I.

The potential describing the interactions between the adsorbed alkanes and the substrate was taken without modification from our work on self-assembled monolayers.[34] We use an external 12-3 potential to represent the bead–surface interaction. The parametrization mimicks the interaction between alkane beads and a flat, structureless Au(111) surface at $z=0$.[34] Our decision to use a *simple* external potential instead of a more refined atomic potential with corrugation is based on two main reasons. First, the external potential results in a substantial increase of the computational efficiency, and second, the corrugations on the Au(111) surface should be small and therefore should not be pivotal for the outcome of the simulations. As discussed later, this statement is supported by comparison of our results with simulations studies where the substrate was treated atomistically. Details of the external bead–substrate potential can also be found in Table I.

At this point we would like to discuss some of the differences between the bead–substrate potentials used in the present study and by others.[9,35] Thermal desorption experiments have been carried by Sexton and Hughes[36] for the homologous series of *n*-alkanes (ranging from butane to decane) adsorbed on Pt(111) and for a variety of alcohols, esters, and other hydrocarbon derivatives on both Pt(111) and Cu(100), by Salmeron and Somorjai[37] for *n*-butane and *n*-pentane on Pt(111), and by Dai and Gellman[38] for *n*-alkanols on Cu(100). The thermal desorption spectra for the *n*-alkanes show two clearly distinguishable peaks;[36] for a given alkane the peaks at lower and higher temperatures have been identified as multilayer and monolayer peaks, respectively, i.e., the molecules in the monolayer closest to the surface are more strongly adsorbed than the other molecules

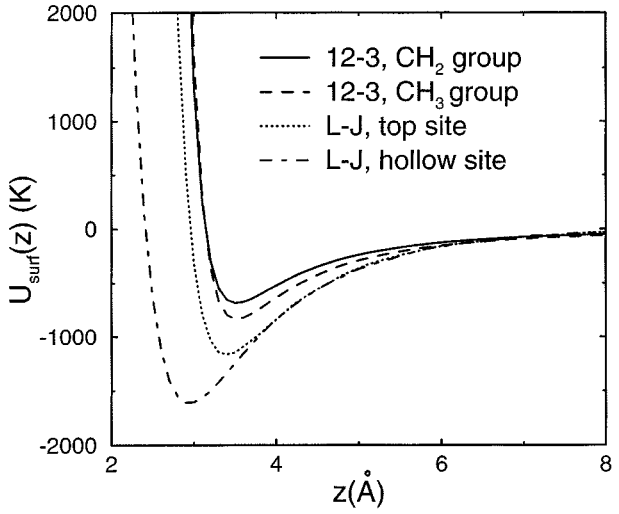

FIG. 1. Interaction potential of methyl and methylene groups (beads) with the surface. The potential used in this work is of the 12-3 form (Ref. 34) (see Table I) with the surface considered to be structureless. The potential employed in Refs. 9 and 11 (a Lennard-Jones function with $\epsilon=216.6$ K and $\sigma=3.28$ Å) for interactions between a bead and a structured Au(100) surface is also shown for comparison (labeled L-J). Three layers of gold atoms as reported in Ref. 9 were used. The spherical interaction cutoff was set to 10.0 Å (Ref. 10).

belonging to multilayer films (thicker films). From the slopes of a plot of the heats of adsorption obtained from the monolayer peaks vs the carbon number, Sexton and Hughes[36] conclude that the heat of adsorption is approximately 5 to 6 kJ/mol per carbon unit. They conclude that the increase per carbon unit is similar for the *n*-alkanes and the alkane derivatives (when the alkyl tails are sufficiently long) and that the differences between the two metal surfaces [Pt(111) and Cu(100)] are small. Similarly, Dai and Gellman[38] obtained a value of 5.0 kJ/mol per carbon unit from submonolayer coverage of *n*-alkanols on Cu(100).

Figure 1 shows the potential curve for the interaction of a single carbon bead with our external 12-3 potential. The well depth for the CH_2 unit is 683 K (or 5.68 kJ/mol). However, this value does not automatically imply that the per-unit increase in the heat of adsorption of the alkanes is correctly described by our potential. Therefore, we have evaluated the heat of adsorption of a single *n*-hexadecane molecule at $T=350$ K using the energies of the adsorbed molecule and of the molecule in its gas phase. The isosteric heat of adsorption defined as the difference between the molar enthalpy of the gas-phase molecule and the partial molar enthalpy of the adsorbed molecule, is calculated from the following expression[15,39]

$$Q_{\mathrm{st}}=-[\langle U_{\mathrm{adsorbed}}\rangle-\langle U_{\mathrm{ideal\ gas}}\rangle-k_BT].$$

The outcomes of the test simulations for a single molecule are summarized in Table II. The heat of adsorption is found to be approximately 84 kJ/mol most of it originating from the bead–substrate potential, but an additional small contribution arising from a lower torsional energy of the adsorbed molecule. From this, we can estimate that the incremental heat of adsorption per carbon unit is approximately 5.2 kJ/mol (or 630 K). This value is in very good agreement with

TABLE II. Comparison of the potential energy contributions and heats of adsorption calculated for a single molecule at $T=350$ K using our external potential, the atomistic potential of Xia *et al.* (Ref. 9 and 11) and that used by Fichthorn *et al.* (Ref. 35 and 40).

	Our substrate	Xia's substrate	Fichthorn's substrate	Gas phase
$\langle U_{\mathrm{stretch}}\rangle$/K	2642±5	2637±6	2663±40	2628±6
$\langle U_{\mathrm{bend}}\rangle$/K	2422±5	2414±6	2447±34	2445±6
$\langle U_{\mathrm{torsion}}\rangle$/K	3477±7	2912±7	2918±52	4527±7
$\langle U_{\mathrm{LJ}}\rangle$/K	−740±1	−690±1	−682±6	−869±2
$\langle U_{\mathrm{subs}}\rangle$/K	−8792±5	−19449±6	−14633±37	0
$\langle U_{\mathrm{total}}\rangle$/K	−991±13	−12176±14	−7286±94	8731±11
Q_{st}/K	10070±20	21260±20	16400±100	···
Q_{st}/kJ/mol	83.7±0.2	176.7±0.2	136±1	···

the experimental value for submonolayer coverages,[38] and should be lower than the value obtained from the thermal desorption experiments by Sexton and Hughes,[36] since those apply to monolayer coverages and the interaction with the other molecules in a monolayer will lead to an increase of the heat of adsorption. Thus our value of 5.2 kJ/mol marks only the lower bound for monolayer coverages. The monolayer heat of adsorption for our potential model can also be estimated following a different route. We have simulated multilayer films of different thicknesses (see later) and we might be able to extrapolate the heats of adsorption of these multilayers to that of a monolayer. For the 10, 15, 20, and 40 Å thick films at 350 K we have obtained the following mean energies (heats of adsorption in brackets) per molecule: −11.9 (87.9), −5.3 (81.3), 0.6 (75.4), and 2.6 (73.4) kJ/mol, respectively. Already, the per bead value of 5.5 kJ/mol for the thinnest film is larger than the value estimated for the single molecule. From this discussion, it is clear that the adsorption energies resulting from our external potential fall within the range of the experimentally estimated adsorption energies.

Since one of our goals is to compare our results to recent simulation studies on related systems, it is helpful to describe the potentials used by others. Xia *et al.*[9,11] have previously studied multilayer films of *n*-hexadecane, but they use an atomistic model to described a static, crystalline Au(100) surface. The interaction between the united atoms of the adsorbed alkane molecules (no distinction is made between CH_2 and CH_3 groups) and three layers of gold atoms is governed by a Lennard-Jones potential with parameters $\sigma=3.28$ Å and $\epsilon=1.795$ kJ/mol (or 216 K).[9] Xia *et al.* report that this potential was chosen to yield an adsorption energy of approximately 4 kJ/mol per *pseudo*-atom unit. However, considering that for adsorption at the preferred hollow site, a carbon unit can directly interact with four gold atoms, the ϵ value chosen by Xia *et al.* seems rather large. It is instructive to calculate the potential for a single *pseudo*-atom adsorbed on a top and hollow site of the Au(100) surface (see Fig. 1). The calculated well depths are a factor of 2 (top site) or 3 (hollow site) larger than the well depths of our external potential for the CH_2 group. We have also calculated the heat of adsorption for *n*-hexadecane following the same route as described above (see Table II). For the single *n*-hexadecane

TABLE III. Details of films studied. N denotes the number of molecules, x,y is the edge length of the square base of the simulation cell, $(h,\perp)$ in the fourth column indicates that the molecules were arranged in the herringbone structure with their long axes perpendicular to the substrate (see text).

N	x,y (Å)	Film thickness at 350 K (Å)	Initial configuration at 350 K	Symbol
48	61.2	10	$h,\perp$	R_{10}^{350}
72	61.2	15	$h,\perp$	R_{15}^{350}
144	61.2	20	$h,\perp$	R_{20}^{350}
144	43.275	40	liquid	R_{40}^{350}

molecule the mean energy resulting from bead–substrate interactions is found to be a factor of 2 larger for the potential of Xia *et al.*, and the torsional energy is further reduced with respect to the gas phase molecule. The resulting heat of adsorption is 180 kJ/mol (or, 11 kJ/mol per carbon unit), i.e., a factor of 2 larger than the experimental heat of adsorption and also much larger than the value reported by Xia *et al.* for their model.[9,11] The present external potential, albeit simpler than the atomistic potential of Xia *et al.*, nevertheless gives a much better description of the measured strength of the physisorption of alkanes on metal surfaces.

Fichthorn and co-workers[35,40] have carried out a simulation study of butane on Pt(111) using an atomistic description of the substrate and a Lennard-Jones potential for the bead–substrate interactions. The interaction between the united atoms of the adsorbed alkane molecules (no distinction is made between CH_2 and CH_3 groups) and five layers of platinum atoms is governed by a Lennard-Jones potential with parameters $\sigma=3.231$ Å and $\epsilon=1.30$ kJ/mol (or 156 K).[40] A potential truncation at 2.5σ is employed. Fichthorn *et al.*[40] report that this choice of alkane–substrate potential will approximately reproduce the experimental heat of adsorption for *n*-butane on Pt(111) of 34.3 kJ/mol.[37] We have also calculated the heat of adsorption for a single *n*-hexadecane molecule using this model (see Table II). The value of $Q_{st}=136$ kJ/mol is exactly four times larger than that calculated for *n*-butane by Fichthorn *et al.* Therefore, we can be assured that the discrepancies found for the heat of adsorption for the model of Xia *et al.* (see previous paragraph) are not caused by a programming error on our side. Due to the fact that Fichthorn *et al.* neglect the differences between methyl and methylene groups, their alkane–substrate potential yields an overestimate of the heats of adsorption for the longer alkanes (the per carbon unit contribution is 8.5 kJ/mol instead of the experimentally observed 5 to 6 kJ/mol). In principle, it will be very simple to adjust the parameters in Fichthorn's alkane–substrate potential to obtain a good description of both short and long alkanes.

III. SIMULATION DETAILS

We have studied four liquid films whose nominal thicknesses ranged from 10 to 40 Å. Some details of the runs carried out here are described in Table III. Periodic boundary conditions were applied in the x and y directions. For the thinner films, the chains were initially stacked in the form of ordered layers. Within these layers, the chains in their all-*trans* conformation were arranged in a hexagonal packing with their long axes perpendicular to the substrate and their carbon backbone planes in a herringbone pattern. The initial configuration for the 40 Å film was obtained from a MC run of bulk liquid hexadecane which was then placed on top of the substrate at a distance sufficiently large to avoid severe overlaps (repulsive interactions between chains and substrate). In this respect, the latter is similar to the simulations carried out by Xia *et al.*[9] in which the starting configurations for all films were obtained from runs of bulk liquids. It should be emphasized here that the initial configurations of our films (chains standing perpendicular to the surface and containing no conformational defects) are far removed from their equilibrated structures (chains lying flat on the surface with a substantial number of defects).

During each Monte Carlo step, a molecule and a type of move were selected at random. As in our previous studies for self-assembled monolayers,[41] we have used three different types of moves: (i) translation of the molecule, (ii) rotation of the molecule around the central bead, and (iii) the partial or full regrowing of the molecule by the CBMC method. Moves (i) and (ii) do not change the internal conformation of the molecule. N such steps constitutes a MC cycle. Typical equilibration lengths (for the runs at $T=350$ K starting from the initial configurations described above) were around 30 000 cycles for the thinner films to around 100 000 cycles for the thicker ones. Equilibration has been very carefully monitored by calculating a range of quantities, including the mean energy of the adsorbed chains, the bead density profiles, the number of beads in the first layer, the orientational distribution of the molecules, the distribution of conformational defects, etc. After all test showed that the samples were well equilibrated, the production part of the runs were started. Most of the properties reported in the next section were averaged over at least 50 000 cycles in each run. (The CPU time needed for a 1000 cycle run of the thickest film on a HP 735 workstation was around 4 h).

In addition to the simulations at $T=350$ K, further calculations were performed for all four film thicknesses at 450 and 550 K. The 15 Å film was also studied at 650 K. Simulations at higher temperatures were started from the final configurations of films containing the same number of molecules at the preceding lower temperature which allowed us to reduce the equilibration periods for these runs. It should be noted that the melting and boiling temperatures (at atmospheric pressure) of bulk liquid hexadecane are around 291 and 560 K, respectively.[42] The following notation is used henceforth to specify the systems studied: R_t^T denotes a simulation run at temperature T, in Kelvin, for the film whose thickness at 350 K was t Å.

IV. RESULTS AND DISCUSSION

A. Molecular packing

As already noted from the appearance of the distinguishable monolayer and multilayer peaks in the thermal desorption experiments,[36] the interaction between the hydrocarbons and the substrate is stronger than that between the hydrocarbons themselves. Similarly in our case, the well depth for the

external 12-3 potential is much larger than the well depths of the Lennard-Jones potentials for the hydrocarbon interactions. However, these values should not be compared directly because of the different functional forms and the fact that the external potential, of course, mimicks the interaction with an array of metal atoms. As a consequence, the molecules have a strong preference to arrange themselves parallel to the surface to maximize the number of beads close to the surface. This leads to the formation of a dense ''monolayer'' next to the surface. The presence of this compact first layer induces another, well discernible layer on top of it. Further away from the substrate the layering becomes weaker and weaker. This layering of molecules is evident from the snapshots of the final configurations of runs R_{15}^{350} and R_{40}^{350} shown in Fig. 2.

The bead density profile for run R_{40}^{350} (see Fig. 2) exhibits three (or, maybe, four) discernible peaks giving evidence for the existence of at least three layers of molecules above the surface. The peaks are separated by about 4.5 Å. This is roughly the same as the spacing found in crystalline alkanes[43] and is consistent with what we may expect from the minimum energy separation of two methylene groups ($2^{1/6}\sigma$=4.41 Å). The present results are in good agreement with the experimental data of Christenson *et al.*[3] who observed oscillations with similar spacing in the force profiles of alkanes confined between mica surfaces. A striking feature of the bead density profiles shown in Fig. 2 is that the characteristics of the first peak remain virtually unchanged for films of different thicknesses.[44] Thus, the average density of chains in the first layer is substantially independent of the existence of molecules above it. This is, in a sense, to be expected as the molecule–surface interactions are much stronger than the intermolecular interactions. Hence, once the close packing density of chains in the first layer is achieved (see below), the addition of more molecules above the first layer has only a negligible effect on the density of the layer closest to the surface. Similarly, the bead density profiles of the thicker films (runs R_{20}^{350} and R_{40}^{350}) are not discernibly different up to the third minimum in the density profile (i.e., as far as 15 Å away from the substrate).

The extent of close packing of molecules in the first layer can be judged visually from a snapshot (top view of only the first layer, see Fig. 3). A more quantitative measure is the average density in that layer. For this purpose, only beads with z coordinates less than the first minimum in the bead density profile at each temperature have been considered. The lower z bound of the first layer has been taken somewhat arbitrarily as 3.0 Å, the distance at which the bead density profiles start to exhibit a nonzero value. At 350 K, the average densities in the first layer are found to be around 1.0 g/cm^3 (compared to a value of 1.16 g/cm^3 reported by Xia *et al.*[44]) which is 40% higher than the corresponding density of bulk hexadecane.[43] At 550 K, the average density in the first layer decreases to 0.88 g/cm^3.

It is worth noting that for the thickest film, run R_{40}^{350}, the density of the bulklike part (from approximately 20 to 35 Å) is in very good agreement with the experimentally known bulk density of n-hexadecane (0.73 g/cm^3 at 350 K,[44] indicated by an arrow in Fig. 2). At higher temperatures, the bulk

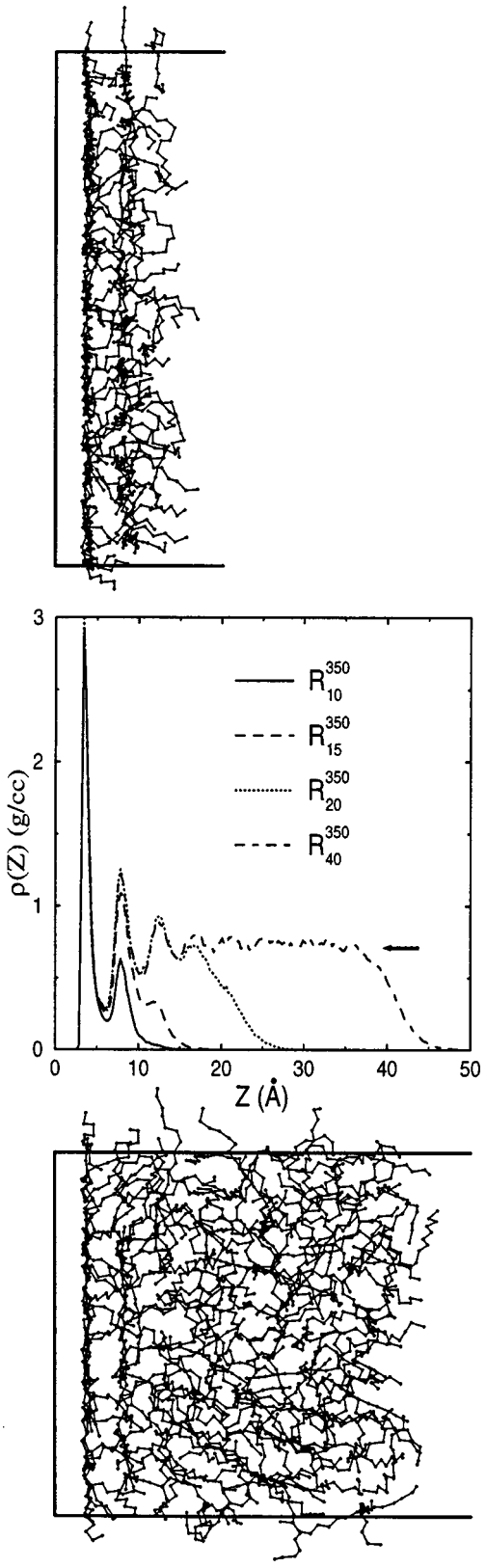

FIG. 2. Bead density profile as a function of the z-coordinate for n-hexadecane films of different thicknesses at T=350 K. Here, z=0 corresponds to the position of the surface. The density profile is sandwiched between snapshots of the final configuration of a 15 Å (top) and a 40 Å thick film. The region between 20 and 30 Å for the thickest film corresponds closely to the bulk liquid density of 0.73 g/cm^3 which is indicated by an arrow.

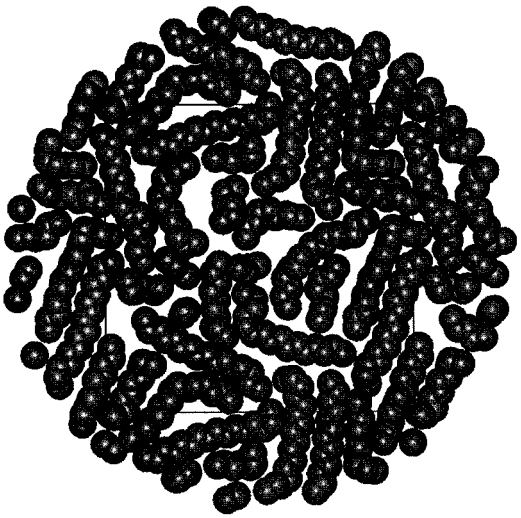

FIG. 3. Snapshot of the top view of molecules in the first layer at 350 K for the 40 Å film along with their periodic images. Bead sizes correspond to their van der Waals radii. The edge length of the square is 43.275 Å. The predominantly zig–zag nature of the chains indicates that the backbone planes are mostly flat on the substrate ($\cos\phi = \pm 1$).

region densities decrease (for example, we find it to be 0.57 g/cm^3 at 550 K), and are always close to the experimental bulk values. In contrast, Xia *et al.*[9,11] using the alkane model of Ryckaert and Bellemans[45] obtain a bulk density of 0.86 g/cm^3 at 350 K, which is more than 15% larger than the experimental value. The fact that the potential model employed here has been constrained by fitting the parameters to liquid–vapor coexistence curves,[31] ensures accurate reproduction of the bulk liquid density over a wide temperature range.

Figure 4 shows the bead density profiles for the 15 Å film at four different temperatures. The average densities of the first layer decrease by about 6% for every 100 K increase in temperature. The liquid film thickens and exhibits a longer tail in the density profiles and the order in the z direction is

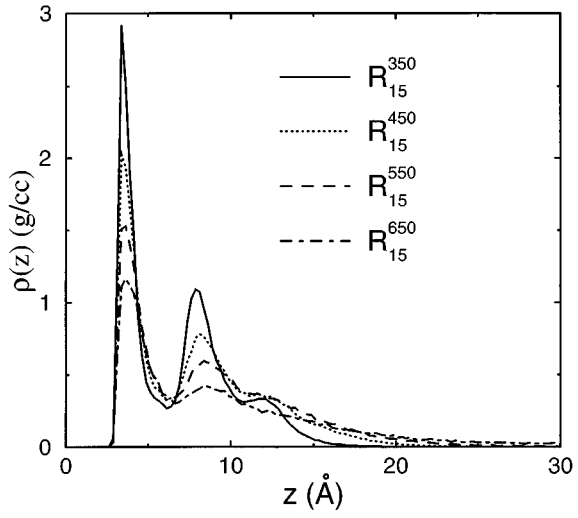

FIG. 4. Bead density profiles for the 15 Å thick hexadecane film at four different temperatures, ranging from 350 to 650 K in steps of 100 K. The height of the first peak decreases with increasing temperature.

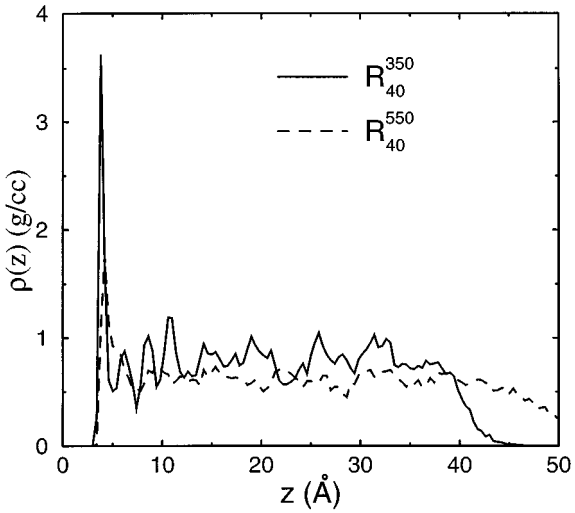

FIG. 5. Density profiles of the center of mass of the molecules at two temperatures for the thickest film.

considerably weakened. The peak positions are also shifted to higher distances due to the increased temperature. At 650 K which is substantially higher than the boiling point of the bulk material, the hexadecane film is not stable and we observed that a noticeable fraction of the molecules in the system irreversibly desorbed from the surface.

The density profile of the individual beads provides information on the layering of these molecules. But, the behavior of a dynamical quantity like the shear viscosity is more likely to be dependent on how compact and how well stratified these layers are. A good measure for this ''compactness'' of the layers may be the density profiles of the center-of-mass (COM) of these molecules which are plotted in Fig. 5 for runs R_{40}^{350} and R_{40}^{550}. In spite of the much poorer statistics for this molecular property, in comparison to the bead density profiles, the COM profiles provide valuable information. At 350 K, the first peak in the COM density profile is much narrower and correspondingly higher than the first peak in the bead density profile, being a clear identification of the compactness of this layer. The peak position of the first peak, however, is very similar in both cases. In contrast, the COM density profile shows a peak at approximately 6 Å, a position where the bead density profile has its first minimum. The third peak of the COM density profile is close in position to the second peak of the bead density profile, and finally there is a fourth discernible peak in the COM density profile at a position close to the second minimum in the bead density profile. At 550 K, only the first peak is prominent and its shape is characterized by a shoulder at higher z values. What is the reason for the additional peaks (and also the shoulder) in the COM density profiles? They are caused by molecules which interdigitate between layers, i.e., have individual CH_2 units in two (or sometimes more) distinct layers. These interdigitating molecules are clearly visible in side views of the films (see Fig. 2) and the ''links'' between the first and second layers belong to them. To better quantify this effect, we have calculated the probability to find a given chain with its center-of-mass in layer l having n_l of its beads in that layer. This quantity is plotted in Fig. 6. At 350 K, about 83% of the

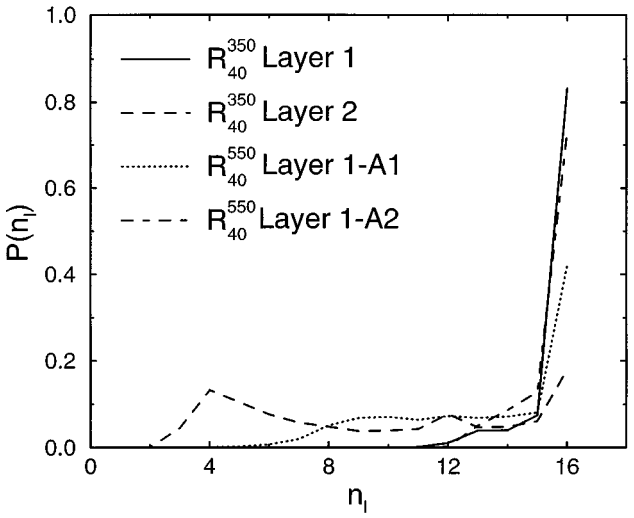

FIG. 6. Interdigitation plot for the 40 Å thick film. The figure indicates the probability of a chain whose center-of-mass is in the lth layer having n_l of its beads in the same layer. The center of mass density profile at 550 K shows a small hump at 5.25 Å while the first minimum is at 7.0 Å (see Fig. 5). The bead density profile (which is used to determine the proportion of beads in the layer) at 550 K exhibits a minimum at 6.25 Å. Thus, the analysis for this run has been performed in two ways. In A1, the cutoff for identifying a chain to be in the first layer (based on its center-of-mass) is taken to be 7.0 Å whereas that in A2, is taken to be 5.25 Å.

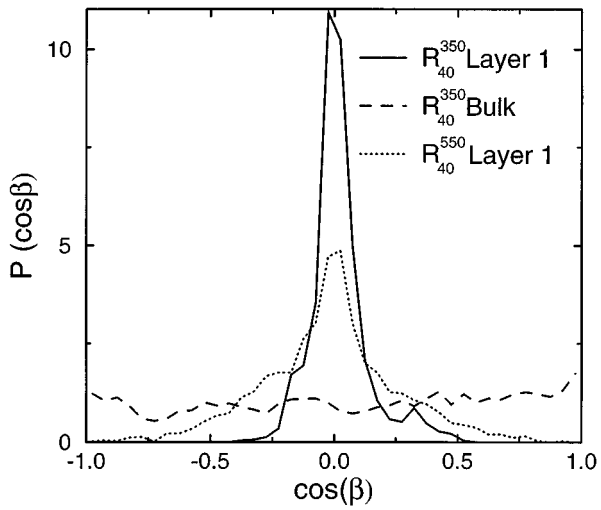

FIG. 7. The distribution of tilt angles (defined as the angle β between the molecular end-to-end vector and the normal to the surface) for molecules in the first layer of a 40 Å film at 350 and 550 K and for those in the bulk region at 350 K.

molecules in the first layer have all their beads in this layer, while only 18% of those in the second layer are found to have all their beads exclusively in the same layer. At 550 K, these values decrease dramatically to 42% and 7%, respectively. Xia *et al.*[9] have found that at 350 K, nearly 78% of the chains in the first layer have both their end beads in the same layer, which is in close agreement with our results. Similarly, in the top view of the first layer of run R_{40}^{350} (see Fig. 3) most of the molecules in the central box are shown complete, i.e., have all their beads in the first layer. Clearly, the compactness of the first layer will have a profound impact on the rheology of confined alkane films.

B. Molecular orientation

We now turn to an examination of the structural properties of the molecules in different layers and compare them with those of the bulk *n*-hexadecane liquid. With this aim, we may define the boundaries of each layer with the help of the COM density profiles (see Fig. 5). We have already pointed out that these density profiles exhibit a sharp first peak with minima at $z=5.0$ Å and 7.0 Å for 350 K and 550 K, respectively. Hence, we take these distances to define the upper bound of the first layer. Molecules with COM between 20 and 30 Å above the surface have been considered to belong to the "bulk" phase.

The side views (see Fig. 2), and the fact that the separations between any two adjacent peaks in the bead density profile are nearly the same as the diameter of a bead, suggests that the molecular axes should be parallel to the surface.[3] This can be verified from the distributions of the tilt angles which are shown in Fig. 7. At 350 K, we find a very sharp distribution for the molecules in the first layer surface which is centered around a tilt angle of 0°, i.e., a overwhelming number of chains are oriented with their long axes parallel to the substrate. The sharpness and peak height for the first layer distribution decreases substantially with increasing temperature, but the distribution remains, nevertheless, far from uniform. In contrast, the orientation of the molecules with COM positioned in the region from 20 and 30 Å appears to be isotropic, thus justifying our use of the term "bulk."

An important problem in the study of adsorbed long chain molecules is how their backbone zig–zag plane is oriented with respect to the surface. The exact orientation of the zig–zag plane in alkane lamellae adsorbed on graphite has been a contentious issue.[17,19–21,46] For linear alkanes, the geometry of adsorbed alkanes on graphite is not only determined by the interchain interactions but is also affected by the periodicity in the basal plane of the substrate as well as the coverage. The surface presently employed is markedly different from any corrugated surface, in that it is structureless. We will see later that our structureless surface prevents us from observing certain orientational ordering which has been observed in other simulation studies on graphite or Au(100).

The backbone plane for an entire hexadecane molecule is well defined only for all-*trans* conformations. Since few of the molecules in our study are all-*trans*, we have used a local description of the zig–zag plane defined to be the plane formed by any three successive beads in a molecule. The angle between these local planes and the substrate can be called the twist angle, ϕ. The reader is cautioned that this definition differs from the ones we have previously used to calculate twist angles in the case of self-assembled and Langmuir–Blodgett monolayers.[34,41,47] The probability distribution of ϕ for various layers and runs is shown in Fig. 8. At 350 K, chains closest to the surface prefer not only to lie flat on the surface (tilt angle of 90°), but also in a way such as to orient their zig–zag plane parallel to the surface (twist angle of 0°). Also the top view shown in Fig. 3 in which the

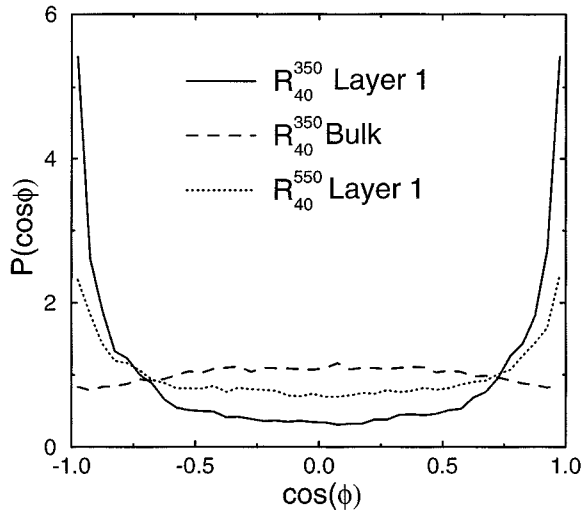

FIG. 8. The distribution of the angle ϕ between the surface and the backbone zig–zag plane.

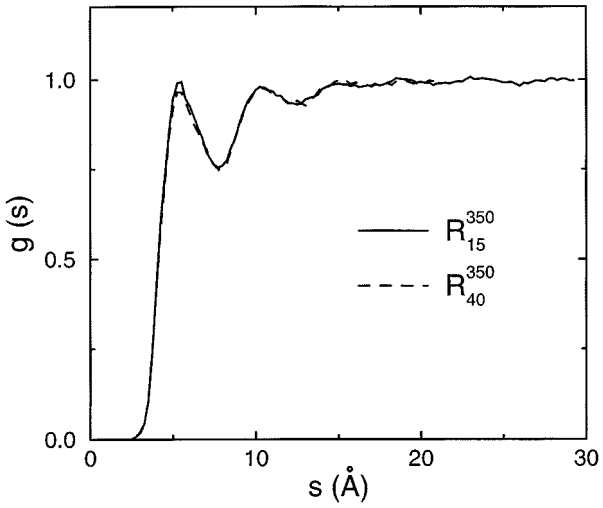

FIG. 9. The two-dimensional pair correlation function $g(s)$, between beads of different molecules in the first adsorbed layer at 350 K for films of two thicknesses. "s" denotes the interbead separation projected on the surface. The nearly identical nature of the curves implies that the in-plane structure of molecules adsorbed in the first layer is essentially *unaffected* by the thickness of the film.

zig–zag nature of the chain backbone is clearly evident gives a good impression that the backbone planes are mostly parallel to the substrate. This arrangement is certainly energetically more favorable in the present situation (i.e., for our uncorrugated surface). Such a parallel orientation of the backbone zig–zag planes has been observed in monolayer and multilayer films of *n*-alkanes on Pt(111) by Firment and Somorjai[48] using low energy electron diffraction. Nuzzo *et al.*,[49] through infrared spectroscopy have also observed a parallel orientation of the backbone zig–zag plane with the substrate in films composed of shorter *n* alkanes on Pt(111) in agreement with the present study. This is an evidence that in this respect our description of the (111) surface does not introduce any gross artifacts. At 550 K, we find that chains in the first layer tend to have less preference for the parallel orientation, while the chains in the bulk phase again have an isotropic distribution.

On a structured surface like graphite, the alkane molecules in the first layer exhibit significant translational and orientational correlations. The melting of monolayers of butane and hexane molecules adsorbed on graphite has been studied by neutron diffraction and molecular dynamics simulations.[50,51] Leggetter and Tildesley[16] have studied the orientational correlations between decane molecules adsorbed on graphite at submonolayer and monolayer coverages. More recently, Xia *et al.*[9] have studied these correlations for hexadecane films on Au(100) surface. These studies suggest significant translational and orientational order between molecules in the first layer up to distances of 20 Å. It would thus be worthwhile to evaluate the in-plane structural correlations between the molecules belonging to the first layer in our study to compare with those obtained from films on structured surfaces. The pair correlation functions between beads belonging to different molecules are shown in Fig. 9 for the 15 and 40 Å films at 350 K. The first peak is located at 5.2 Å, a distance considerably larger than the interbead spacing found in crystalline alkanes and the interlayer spacing in our alkane films. It is noteworthy that the bead radial distribution functions in the first layer are virtually identical for the thin and thick films. This reinforces our previous observations based on the first peaks of the bead density profiles (Fig. 2) that the structure of the first layer is virtually independent from the number of layers on top of it. We profitably employ this feature in the calculation of the radial distribution function of the COM of molecules in the first layer and its circular harmonics. Since this is a function sampling over entire molecules, data pertaining to the 40 Å film (recall the different box dimension for the thickest films) would lead to poorer statistics. Thus, we focus on the data for the 15 Å film at 350 K in the immediately following discussion. In Fig. 10, we observe that $g_{00}(s)$ exhibits a peak

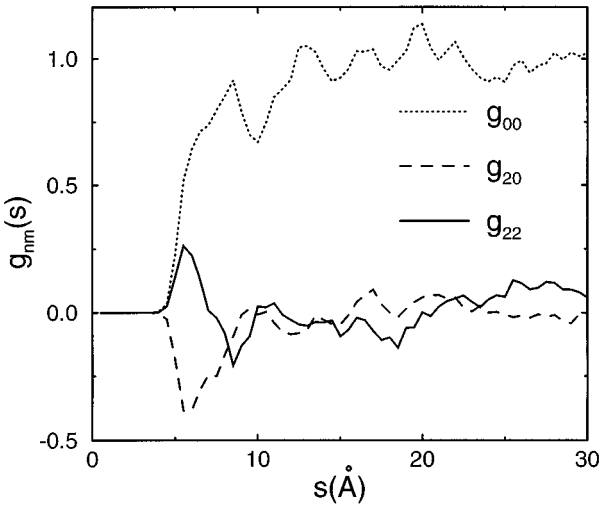

FIG. 10. The radial distribution function (g_{00}) of the center-of-mass of chains in the first layer at 350 K for the 15 Å thick film. s is the magnitude of the projected center of mass vector **s** between two molecules. Also shown are the circular harmonics $g_{20}(s)$ and $g_{22}(s)$ defined as (Ref. 16)
$g_{nm}(s)=g_{00}(s)\langle\cos(n\theta_1)\cos(m\theta_2)-\sin(n\theta_1)\sin(m\theta_2)\rangle_{\text{shell}}$,
where θ_i is the angle between the surface projection of the end-to-end vector of molecule i and **s**.

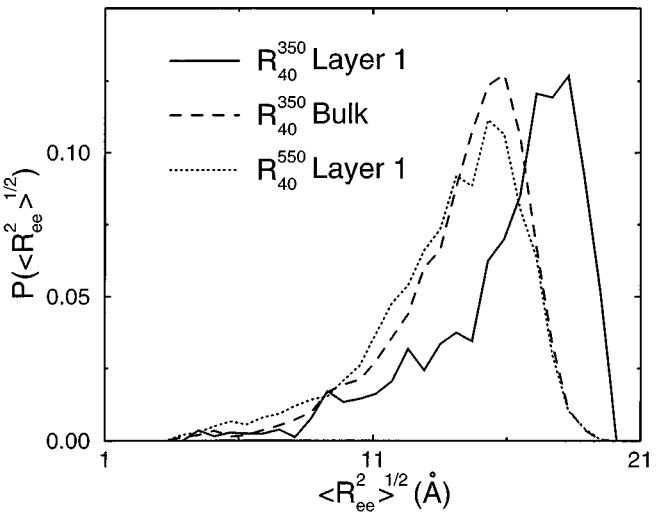

FIG. 11. Probability distribution of the root-mean-squared end-to-end lengths $\langle R_{ee}^2 \rangle^{1/2}$.

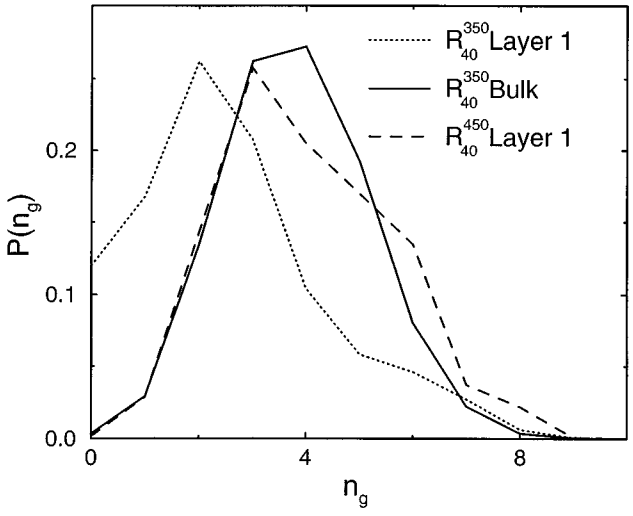

FIG. 12. Probability distribution of the number of *gauche* defects in a chain.

at around 8 Å, most likely arising from nearest-neighbor molecules which have only parts of their long axes aligned with each other. We also detect a small shoulder at smaller separation, which comes from pairs of parallel chains. The first negative peak at $s=6$ Å in $g_{20}(s)$ indicates that pairs of molecules at this spacing have predominantly an orientation perpendicular to the vector connecting their COM. This is supported by the first positive peak in g_{22} also at $s=6$ Å which is caused by parallel intermolecular alignment. The adjacent negative peak at $s=9$ Å indicates pairs of molecules in a T-like arrangement. All these structural features can be distinguished in the snapshot of the first layer (see Fig. 3), and have previously been reported for hexadecane on Au(100).[9] We detect no significant translational and orientational correlations extending further than 10 Å (second-nearest neighbor or T-shape) for our films. This is in marked contrast to simulations on corrugated surfaces. For adsorption of liquid alkane films on atomically modeled Au(100)[9] and graphite[16] surfaces much stronger correlations are found which can extend to distances of 20 Å. Thus, the price we have to pay for our simple external bead–substrate potential is the weakening of these in-plane correlations in the first layer.

C. Molecular conformation

From the distributions of root-mean-square end-to-end lengths of the molecules, $\langle R_{ee}^2 \rangle^{1/2}$ (see Fig. 11), it can be observed that at 350 K, chains in the first layer are much more extended than the molecules in the other layers (also compare the length of an all-*trans* molecule which is 19.4 Å). An increase of temperature results in a pronounced decrease of $\langle R_{ee}^2 \rangle^{1/2}$ and for molecules in the first layer an increase of 200 K leads to a shift of the peak position by approximately 3 Å. Here we should draw the attention of the reader to the striking similarity of the $\langle R_{ee}^2 \rangle^{1/2}$ distributions for the first layer at 550 K and the bulk phase at 350 K. X-ray reflectivity[52] and surface tension[53] measurements on liquid alkane films have shown that alkane molecules in the liquid–vapor (l–v) interface tend to crystallize at a somewhat higher temperature (around 3 K) than the bulk melting temperature. Thus the distribution of end-to-end lengths would be much different in the l–v interface than in the bulk of the film. In our thickest film, molecules whose centers-of-mass was between 38 and 45 Å away from the surface were taken to be part of the l–v interface. The distribution of $\langle R_{ee}^2 \rangle^{1/2}$ in this region was found to be nearly identical to that in the bulk region of the film, probably because our operating temperatures (350 K or higher) are significantly above the bulk melting temperature.

For the relatively short *n*-hexadecane molecules (compared to polymers), there is an intimate relationship between $\langle R_{ee}^2 \rangle^{1/2}$ and the number of conformational defects. Fewer *gauche* defects result in a more extended molecule. The ratios (percentages) of the different types of dihedral angles ($g^-:t:g^+$) for chains in the first layer of run R_{40}^{350} is found to be 10:80:10, whereas at 550 K, it is found to be 18:64:18. We can also observe that at 550 K, the first layer has nearly as many *gauche* defects (36%) as the corresponding bulk liquid. These values are in very good agreement with those reported by Xia *et al.*[9] at 350 K and by Xia and Landman at 550 K.[54] The probability distribution of the number of *gauche* defects in any given chain is shown in Fig. 12 for the first layer and the bulk phase of run R_{40}^{350} and the first layer in run R_{40}^{450}. Though only around 12% of the chains in the first layer at 350 K are in the all-*trans* conformation, and the most probable number of conformational defects is two, we noted above that these molecules are in very extended configurations (see the distributions of $\langle R_{ee}^2 \rangle^{1/2}$ in Fig. 11). This apparently contradictory result can be explained by a detailed look into the locations and types of conformational defects. The probability of finding a *gauche* defect at a certain position along the chain is plotted in Fig. 13. For molecules in the first layer of run R_{40}^{350}, we observe a significant increase in the proportion of *gauche* defects occurring near the end segments compared to the middle ones. An oscillatory feature in the distribution for these molecules denotes the presence of a kink (gtg) defect. In this respect, the alkane mol-

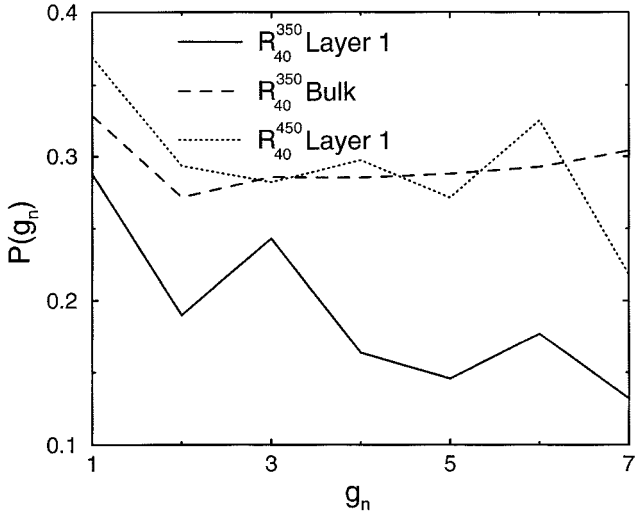

FIG. 13. Probability to find a *gauche* defect at the g_nth dihedral angle from the ends of a chain. The curves are normalized so that their average provides the mean number of *gauche* defects present in that layer. For example, at 350 K, molecules in the bulk liquid have around 30% *gauche* defects.

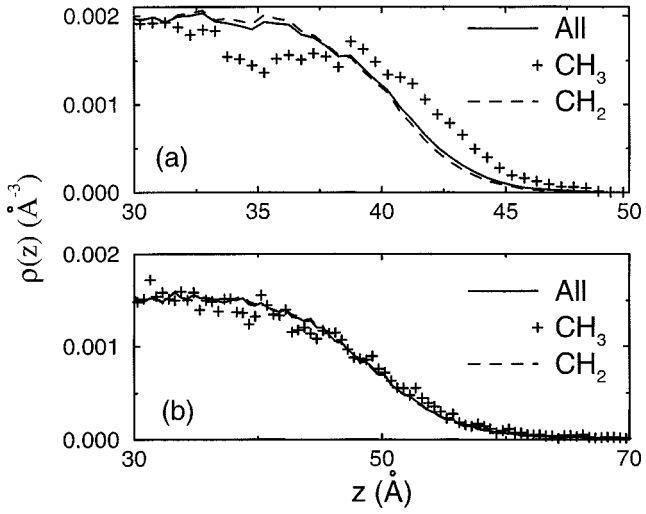

FIG. 14. Normalized individual bead density profiles in the liquid–vapor interface of the 40 Å film at (a) 350 K, and (b) 550 K. There is a dip in the profile of the end segments around 35 Å at 350 K with a corresponding marginal increase for the middle segments. At 550 K, these features are not evident. Notice also that the scale in the abcissae are different in the two graphs.

ecules closest to the solid/liquid interface exhibit features similar to crystalline alkanes[55,56] and the alkyl tails in self assembled monolayers (SAM).[41,57] At higher temperatures or further away from the substrate, molecules contain substantially more conformational defects and do not show any preferential population of *gauche* defects near any portion of the chain. Again, it is surprising to note that the distribution for the first layer at 450 K is similar to that for the bulk at 350 K. Accordingly, this is additional evidence that at higher temperatures, molecules in the first layer begin to exhibit properties similar to those of the bulk liquid at a lower temperature.

D. Liquid–vapor interface

The thin liquid films are not only interesting in their richness of phenomena close to the solid surface, but are also good candidates to study the liquid–vapor interface. Harris has studied in detail the liquid–vapor interface of linear alkanes using molecular dynamics simulations.[13] In particular, for *n*-eicosane at 400 K (which should be similar to our system of *n*-hexadecane at 350 K), a hump in the density profile of the middle segments near the tail region, with a corresponding dip in the density profile of the end segments, was observed in that study.[13] We observe only a marginal increase in the density profile of the middle segments near the tail region, though a pronounced dip in the end segments is observed [see Fig. 14(a)]. The methyl segments have a stronger attraction than the methylene segments (see Table I). Hence, one would expect the end segments to try to bury themselves into the film near the tail region. However, this would entail the creation of some conformational defects in the chain with the associated energetical cost. The position of the end segments is likely to be determined from a competition of these two factors. We find an an excess of end segments on the vapor side of the liquid–vapor interface which might point in the direction that creation of additional *gauche* defects is too costly. It is somewhat puzzling that Harris has observed a noticeable hump in the density profile of the middle segments near the tail region. This seems to be inconsistent with the observation of monotonically decreasing profile for the entire film (see below). At 550 K [Fig. 14(b)] the differences between the contributions from the methylene and methyl groups to the bead density profile vanish, in agreement with the results of Harris[13] as well as with the recent work of Xia and Landman.[54]

The bead density profile at the liquid–vapor interface can be fitted to an error function of the form:[58,9]

$$\rho(z)=0.5(\rho_l+\rho_v)-0.5(\rho_l-\rho_v)\mathrm{erf}((z-z_0)/(2w_\rho^2)^{1/2}.$$

The density profiles and their error function fits at 350 and 550 K are shown in Fig. 15. The fit parameters are found to

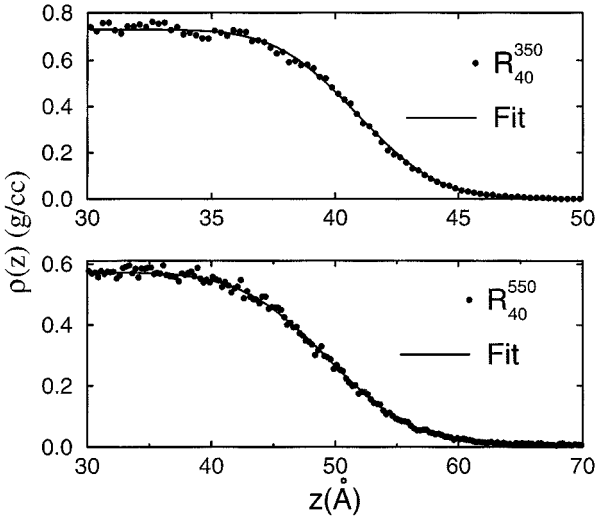

FIG. 15. Error function fits to the tail region of the bead density profile for the 40 Å film at 350 and 550 K. The fit function and the parameters are described in the text.

be w_ρ=2.58 Å and z_0=40.9 Å at 350 K, and 5.53 and 49.4 Å at 550 K, respectively. ρ_v at 550 K (0.0058 g/cm^3) was obtained from vapor–liquid coexistence data.[31] For the same coverage, Xia *et al.*[9] obtain a slightly thicker interface and a thinner film (thinner by 2.3 Å) at 350 K. In addition, at 550 K we obtain a much thicker film (by 5.2 Å) with a liquid–vapor interface width which is slightly larger than that obtained by Xia and Landman.[54] These discrepancies can be explained in terms of their stronger surface interactions and by shortcomings of their alkane model.

V. SUMMARY

In this work, we have investigated in detail the structural properties of liquid *n*-hexadecane films of different thicknesses on a flat, metal surface by the configurational-bias Monte Carlo approach. As in earlier studies, the molecules have been found to adsorb strongly to the surface and are observed to lie with their chain axes and their zig–zag planes parallel to the surface, in good agreement with surface force[3] and spectroscopic[49] data. The average density of molecules in the first layer and the in-plane structure are largely unaffected by the thickness of the film. In this respect, the present results differ with the earlier work of Xia *et al.*[9,11] The densities in the bulk region of the film obtained in the present work compare extremely well with the experimental data both at 350 and 550 K.

At 350 K, the first layer is 40% more dense than the bulk liquid. Density oscillations, arising out of the layering of molecules prevail up to 17 Å above the surface. At the same temperature, molecules in the first layer tend to be more extended, while greater number of *gauche* defects lead to shorter end-to-end lengths in the molecules belonging to other layers. The molecular density profiles at 350 K indicate that the two layers closest to the surface are more compact than the remainder of the film, while at 550 K, only the first layer is found to be so. Chains are able to interdigitate between the distinct layers. In-plane translational and orientational order in the first layer is observed at short distances, but the ordering is substantially weaker than that found in simulation studies using corrugated surfaces. The density profile at the liquid–vapor interface can be described by an error function and the density profile of the methyl segments at 350 K exhibits a nonmonotonic decay near the liquid–vapor interface.

ACKNOWLEDGMENTS

Several stimulating and enlightening discussions with Kari Laasonen, Chris Mundy, and Preston Moore are gratefully acknowledged. We would like to thank Ralph Nuzzo for sharing his results on alkane/Pt(111) systems with us prior to publication, and Dixie Goins, Bill Moehle, Burney Lee, and Paul Kung for their encouragement. The work described herein was in part supported by the National Science Foundation and Albemarle Corporation. J.I.S. acknowledges additional support by the Camille and Henry Dreyfus New Faculty Awards Program.

[1] J. N. Israelachvili, *Intermolecular and Surface Forces* (Academic, New York, 1985).
[2] J. N. Israelachvili, P. M. McGuiggan, and A. M. Homola, Science **240**, 189 (1988).
[3] H. K. Christenson, D. W. R. Gruen, R. G. Horn, and J. N. Israelachvili, J. Chem. Phys. **87**, 1834 (1989).
[4] S. K. Kumar, M. Vacatello, and D. Y. Yoon, J. Chem. Phys. **89**, 5209 (1988); M. Vacatello, D. Y. Yoon, and B. C. Laskowski, *ibid*. **93**, 779 (1990).
[5] M. L. Gee, P. M. McGuiggan, J. N. Israelachvili, and A. M. Homola, J. Chem. Phys. **93**, 1895 (1990).
[6] M. Schoen, C. L. Rhykerd, Jr., D. J. Diestler, and J. H. Cushman, Science **245**, 1223 (1989); M. Schoen, D. J. Diestler, and J. H. Cushman, J. Chem. Phys. **87**, 5464 (1987); **101**, 6865 (1994).
[7] S. Granick, Science **253**, 1374 (1991).
[8] S. Granick, in *Fundamentals of Friction: Macroscopic and Microscopic Processes, NATO ASI Conf. Proc. Ser. E, Vol. 220*, edited by I. L Singer and H. M. Pollock (Kluwer Academic, New York, 1992).
[9] T. K. Xia, J. Quyang, M. W. Ribarsky, and U. Landman, Phys. Rev. Lett. **69**, 1967 (1992).
[10] M. W. Ribarsky and U. Landman, J. Chem. Phys. **97**, 1937 (1992).
[11] T. K. Xia and U. Landman, Science **261**, 1310 (1993); Phys. Rev. B **48**, 11313 (1993).
[12] P. A. Thompson and M. O. Robbins, Science **250**, 792 (1990).
[13] J. G. Harris, J. Phys. Chem. **96**, 5077 (1992).
[14] Y. Wang, Y. K. Hill, and J. G. Harris, J. Chem. Phys. **100**, 3276 (1994).
[15] B. Smit and J. I. Siepmann, Science **264**, 1118 (1994); J. Phys. Chem. **98**, 8442 (1994).
[16] S. Leggetter and D. J. Tildesley, Mol. Phys. **68**, 519 (1989).
[17] R. Hentschke, B. L. Schürmann, and J. P. Rabe, J. Chem. Phys. **96**, 6213 (1992).
[18] P. Padilla and S. Toxvaerd, J. Chem. Phys. **101**, 1490 (1994).
[19] G. C. McGonigal, R. H. Bernhardt, and D. J. Thomson, Appl. Phys. Lett. **57**, 28 (1990).
[20] J. P. Rabe and S. Buchholz, Science **253**, 424 (1991); L. Askadskaya and J. P. Rabe, Phys. Rev. Lett. **69**, 1395 (1992).
[21] G. Watel, F. Thibaudau, and J. Cousty, Surf. Sci. Lett. **281**, L297 (1993).
[22] H.-W. Hu, G. A. Carson, and S. Granick, Phys. Rev. Lett. **66**, 2758 (1991).
[23] J. V. Alsten and S. Granick, Langmuir **6**, 876 (1990).
[24] L. Bocquet and J. L. Barrat, Phys. Rev. Lett. **70**, 2726 (1993); Phys. Rev. E **49**, 3079 (1994).
[25] I. A. Bitsanis and C. Pan, J. Chem. Phys. **99**, 5520 (1993).
[26] J. I. Siepmann and D. Frenkel, Mol. Phys. **75**, 59 (1992); J. I. Siepmann, in *Computer Simulation of Biomolecular Systems: Theoretical and Experimental Applications Vol. II*, edited by W. F. van Gunsteren, P. K. Weiner, and A. J. Wilkinson (Escom Science, Leiden, 1993).
[27] D. Frenkel, G. C. A. M. Mooij, and B. Smit, J. Phys. Condens. Matt. **4**, 3053 (1992).
[28] J. J. de Pablo, M. Laso, and U. W. Suter, J. Chem. Phys. **96**, 6157 (1992).
[29] M. P. Allen and D. J. Tildesley, *Computer Simulation of Liquids* (Clarendon, Oxford, 1987).
[30] J. I. Siepmann and I. R. McDonald, Mol. Phys. **75**, 255 (1992); Phys. Rev. Lett. **70**, 453 (1993).
[31] J. I. Siepmann, S. Karaborni, and B. Smit, Nature **365**, 330 (1993).
[32] B. Smit, S. Karaborni, and J. I. Siepmann, J. Chem. Phys. **102**, 2126 (1995).
[33] C. J. Mundy, J. I. Siepmann, and M. L. Klein, J. Chem. Phys. **102**, 3376 (1995).
[34] J. Hautman and M. L. Klein, J. Chem. Phys. **91**, 4994 (1989).
[35] K. A. Fichthorn, P. G. Balan, and Y. Chen, Surf. Sci. **317**, 37 (1994).
[36] B. A. Sexton and A. E. Hughes, Surf. Sci. **140**, 227 (1984).
[37] M. Salmeron and G. A. Somorjai, J. Phys. Chem. **85**, 3840 (1981).
[38] Q. Dai and A. J. Gellman, J. Phys. Chem. **97**, 10783 (1993).
[39] G. B. Wood, A. Z. Panagiotopoulos, and J. S. Rowlinson, Mol. Phys. **63**, 49 (1988).
[40] D. Huang, P. G. Balan, Y. Chen, and K. A. Fichthorn, Mol. Simulations **13**, 285 (1994).
[41] J. I. Siepmann and I. R. McDonald, Mol. Phys. **79**, 457 (1993).
[42] *CRC Handbook of Chemistry and Physics* (CRC, Boca Raton, FL, 1986).
[43] D. M. Small, *The Physical Chemistry of Lipids* (Plenum, New York, 1988).
[44] Figure 1 of Xia *et al.* (Ref. 9) shows an *increase* in the height of the first peak of the bead density profile with decreasing film thickness. However, at a later point in the same paper, the authors report a constant density of

the first layer independent of the film thickness. This discrepancy is most likely caused by a problem with the plotting of the density profiles in their Fig. 1 [U. Landman, private communication].
[45] J. P. Ryckaert and A. Bellemans, Discuss. Faraday Soc. **66**, 95 (1978).
[46] S. N. Magonov and M.-H. Whangbo, Adv. Mater. **6**, 355 (1994).
[47] J. P. Bareman and M. L. Klein, J. Phys. Chem. **94**, 5202 (1990).
[48] L. E. Firment and G. A. Somorjai, J. Chem. Phys. **66**, 2901 (1977).
[49] R. G. Nuzzo (private communication).
[50] F. Y. Hansen and H. Taub, Phys. Rev. Lett. **69**, 652 (1992).
[51] F. Y. Hansen, J. C. Newton, and H. Taub, J. Chem. Phys. **98**, 4128 (1993).
[52] X. Z. Wu, E. B. Sirota, S. K. Sinha, B. M. Ocko, and M. Deutsch, Phys. Rev. Lett. **70**, 958 (1993).
[53] J. C. Earnshaw and C. J. Hughes, Phys. Rev. A **46**, R4494 (1992); X. Z. Wu, B. M. Ocko, E. B. Sirota, S. K. Sinha, M. Deutsch, B. H. Cao, and M. W. Kim, Science **261**, 1018 (1993).
[54] T. K. Xia and U. Landman, J. Chem. Phys. **101**, 2498 (1994).
[55] M. Maroncelli, H. L. Strauss, and R. G. Snyder, J. Chem. Phys. **82**, 2811 (1985).
[56] J. P. Ryckaert, I. R. McDonald, and M. L. Klein, Mol. Phys. **67**, 957 (1989).
[57] W. Mar and M. L. Klein, Langmuir **10**, 188 (1994).
[58] J. D. Weeks, J. Chem. Phys. **67**, 3106 (1977).
[59] R. E. Reiher, Ph.D. thesis, Harvard University, Cambridge, MA (1985).
[60] P. van der Ploeg and H. J. C. Berendsen, J. Chem. Phys. **76**, 3271 (1982).
[61] W. L. Jorgenson, J. D. Madura, and C. J. Swenson, J. Am. Chem. Soc. **106**, 6638 (1984).